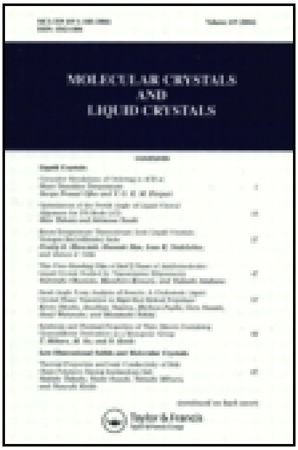

Molecular Crystals and Liquid Crystals
Publication details, including instructions for authors and subscription information:
http://www.tandfonline.com/loi/gmcl20

Synthesis and Optical Properties of Luminescent Naphthalene-based Liquid Crystals

Takeshi Mori [a] & Masashi Kijima [a]

[a] Institute of Materials Science, Graduate School of Pure and Applied Sciences, University of Tsukuba, Tsukuba, Ibaraki, Japan

Version of record first published: 05 Apr 2011

To cite this article: Takeshi Mori & Masashi Kijima (2008): Synthesis and Optical Properties of Luminescent Naphthalene-based Liquid Crystals, Molecular Crystals and Liquid Crystals, 489:1, 246/[572]-256/[582]

To link to this article: http://dx.doi.org/10.1080/15421400802219254

Mol. Cryst. Liq. Cryst., Vol. 489, pp. 246/[572]–256/[582], 2008
Copyright © Taylor & Francis Group, LLC
ISSN: 1542-1406 print/1563-5287 online
DOI: 10.1080/15421400802219254

Synthesis and Optical Properties of Luminescent Naphthalene-based Liquid Crystals

Takeshi Mori and Masashi Kijima
Institute of Materials Science, Graduate School of Pure and Applied Sciences, University of Tsukuba, Tsukuba, Ibaraki, Japan

Luminescent naphthalene-based liquid crystals were newly synthesized and changes of the luminescent color through the phase transitions were characterized. We prepared the compounds by combining naphthalene and known mesogenic cores, oxadiazole and fluorocyanobiphenyl, using methylene spacers. Both oxadiazole-naphthalene and fluorocyanobiphenyl-naphthalene series showed bluish luminescence in all phases. Among them, the emission peaks of 3-fluoro-4-cyano-4′-[8-(6-hexyloxy-2-naphthyloxy)octyloxy]biphenyl in the liquid crystal and isotropic liquid states showed significant red shifts compared to that in the crystal state, which was due to specific interaction between the electron rich naphthalene and electron deficient fluorocyanobiphenyl cores.

Keywords: cyanobiphenyl; naphthalene; oxadiazole; photoluminescence; UV-vis absorption

INTRODUCTION

Liquid crystals have a specific property of self-organization in microdomains, which can lead to macroscopic orientation of molecules. Luminescent molecules having liquid crystalline property could be utilized as intelligent materials functioning as polarized emission, organic lasers, sensors and so on in novel optical and organic semiconductor devices [1]. Up to the present, a variety of luminescent liquid crystals has been reported, and some of them were applied to organic light emitting diodes (OLEDs) [2–14]. The conjugated polymers such

This work was financially supported by the Sasagawa Scientific Research Grant from The Japan Science Society. We would like to thank Chemical Analysis Division, University of Tsukuba, for NMR, PL spectroscopic and elemental analysis data.

Address correspondence to Masashi Kijima, Institute of Materials Science, Graduate School of Pure and Applied Sciences, University of Tsukuba, Tsukaba, Ibaraki, 305-8573, Japan. E-mail: kijima@ims.tsukuba.ac.jp

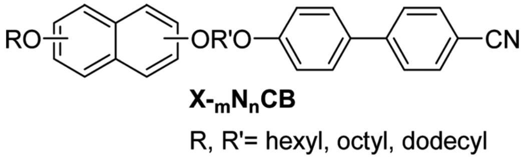

FIGURE 1 The structure of **X-$_{\mathbf{m}}$N$_{\mathbf{n}}$CB** series where X (15, 26), m and n (6, 8, 10) represent the linkage positions (1,5-, 2,6-) of naphthalene core, carbon numbers of alkyl chains at the molecular terminal and inside, respectively.

as polyfluorenes and poly(*p*-phenylenevinylene)s that fluoresced efficient in the solid state succeeded to develop polarized OLEDs by the chain alignment [15–17]. However, reorientation of the emitting material by an external force was not possible because of their specific rigid polymer chain. We have studied to develop a novel emitting device whose emitting property can be controlled by an external force such as temperature, light, electric field, and magnetic field. We have recently reported some photoluminescent naphthalene-based liquid crystals (Figure 1) which showed bluish emission in crystal, liquid crystal and isotropic liquid states, and a significant red shift of the fluorescence spectrum in the liquid crystal state was observed [18]. However, their liquid crystal phases were unstable for further investigations of optical properties of the liquid crystals. From that standpoint, we focused on the synthesis of naphthalene-based liquid crystals having more stable liquid crystalline phases to confirm the spectral change of fluorescence through phase transitions. In this study, we introduce two kinds of mesogenic cores, oxadiazole and fluorocyanobiphenyl, into dialkoxynaphthalenes. The linkage used in these syntheses is limited to ether, because the others such as ester having carbonyl group will be unstable during operation when these materials are used in devices such as OLEDs. In addition, the introduction of such polar mesogenic moiety will have a significance to assist carrier injections.

EXPERIMENTAL

Measurements

UV-vis and photoluminescent (PL) spectra of the naphthalene derivatives in $CHCl_3$ and in the crystal, liquid crystal and isotropic liquid states sandwiched between quartz glasses with a temperature controller were recorded on a U-3500 spectrophotometer (Hitachi) and a FP-750 spectrofluorometer (Jasco). The thermal properties under argon were investigated by a Extra-6000 differential scanning calorimetry (DSC) system (Seiko) at a scanning rate of 10°C/min in the heating and cooling cycles. The textures of mesophases were observed by a polarized optical microscope (POM) equipped with a temperature controller.

Materials

General Procedure for Oxadiazole-Naphthalene (X-$_m$N$_n$Ox) Series

4’-Hydroxybiphenyl-4-carboxylic acid methyl ester **1** (0.300 g, 1.31 mmol) and K_2CO_3 (0.272 g, 1.97 mmol) in DMF (2.00 ml) were reacted at 100°C for 10 min. To the reaction mixture was added dropwise 1-bromooctane (0.380 g, 1.97 mmol), which was stirred at 100°C overnight. The reaction mixture poured into cold water was stirred at room temperature (r.t.) overnight. After the filtration, a white solid was obtained. The resulting white solid (0.420 g, 1.23 mmol) in KOH aqueous solution (5%, 13 ml) and EtOH (30 ml) was heated under reflux for 26 h. After the mixture was cooled to r.t., 12 M HCl was added to neutralize the solution. The resulting white solid was filtered off, giving **2** (0.380 g, 95%).

The compound **2** (0.330 g, 1.01 mmol) and $SOCl_2$ (0.515 ml, 7.06 mmol) in toluene (1 ml) were stirred at 100°C for 26 h. After removing the remaining $SOCl_2$ in vacuo, a white solid of **3** (0.340 g, 98%) was obtained.

The compound **3** (0.300 g, 0.870 mmol) in THF (2 ml) was added dropwise to a solution of 4-benzoic acid hydrazide (0.132 g, 0.870 mmol) in THF (2 ml) and Na_2CO_3 (0.0922 g, 0.870 mmol) in water (2 ml). The reaction mixture was stirred at r.t. overnight, and then poured into water. The resulting white solid was filtered and washed with water to give **4** (0.380 g, 95%).

A solution of **4** (0.350 g, 0.760 mmol), $SOCl_2$ (0.554 ml, 7.60 mmol) and pyridine (0.0125 ml, 0.154 mmol) in toluene (2 ml) was stirred at 85°C for 21 h. The reaction mixture was cooled to r.t. and extracted with EtOAc/water. The organic layer was dried over Na_2SO_4, evaporated in vacuo to give **5** (0.290 g, 86%).

To a stirred solution of **5** (0.500 g, 1.13 mmol), 6-bromo-hexane-1-ol (0.308 g, 1.70 mmol) and PPh_3 (0.446 g, 1.70 mmol) in dry THF (5 ml), diethyl azodicarboxylate (DEAD) (40% in toluene: 0.296 g, 1.70 mmol) was added dropwise under argon at 0°C. The reaction mixture was stirred at r.t. for 25 h, then extracted with CH_2Cl_2/water. The organic layer was dried over Na_2SO_4, evaporated in vacuo. The residue was purified on a silica gel column (EtOAc/hexane: 1/1), then recrystallized from EtOAc to give **6** (0.500 g, 76%).

To a stirred solution of 6-hexyloxy-2-hydroxynapthalene (0.0506 g, 0.207 mmol), K_2CO_3 (0.0286 g, 0.207 mmol) in dry DMF (3 ml), was added **6** (0.150 g, 0.248 mmol) at 100°C. The reaction mixture was stirred at 100°C for 25 h. The mixture was cooled to room temperature, extracted with CH_2Cl_2/water. The organic layer was dried over Na_2SO_4, evaporated in vacuo. The residue was purified on a silica gel column (CH_2Cl_2/MeOH: 30/1), then recrystallized from $CHCl_3$/hexane to give **15-$_6$N$_6$Ox** (0.130 g, 82%). In a similar way, **26-$_6$N$_6$Ox** and **27-$_6$N$_6$Ox** were obtained in 70 and 82% yields, respectively.

General Procedure for Cyanobiphenyl–Naphthalene Series (X-$_m$N$_n$FCB)

To a stirred solution of 6-hexyloxy-2-hydroxynaphthalene (0.200 g, 0.819 mmol) and K_2CO_3 (0.170 g, 1.23 mmol) in DMF (5 ml), 6-bromohexane-1-ol (0.223 g, 1.23 mmol) was added at 90°C, which was stirred at 90°C for 2 d. The mixture was cooled to r.t., extracted with EtOAc/water. The organic layer was dried over Na_2SO_4, evaporated in vacuo. The residue was purified on a silica gel column (EtOAc/hexane: 1/1), then recrystallized from hexane to give a white solid **9** (0.180 g, 64%). To a stirred solution of **9** (0.130 g, 0.377 mmol), 3-fluoro-4'-hydroxy-4-cyanobiphenyl (0.0670 g, 0.314 mmol) and PPh_3 (0.0823 g, 0.314 mmol) in dry THF (3 ml), DEAD (40% in toluene: 0.0547 g, 0.314 mmol) were added dropwise under argon at 0°C. The reaction mixture was stirred at room temperature overnight, then extracted with EtOAc/water. The organic layer was dried over Na_2SO_4, evaporated in vacuo. The residue was purified on a silica gel column (EtOAc/hexane: 1/1), then recrystallized from hexane to give a white solid of **26-$_6$N$_6$FCB** (0.140 g, 80%). In a similar way, **15-$_6$N$_8$FCB** and **26-$_6$N$_8$FCB** were obtained in 14 and 80% yields, respectively.

RESULTS AND DISCUSSION

Synthesis

Oxadiazole-naphthalene derivatives abbreviated as **X-$_m$N$_n$Ox** were synthesized according to Scheme 1, where X represents the linkage positions (1,5-, 2,6-, and 2,7-) of naphthalene core and m and n correspond to carbon numbers of alkyl chains at molecular terminal and inside, respectively. Hydroxylphenyloxadiazole (**5**) was prepared from hydroxybiphenyl derivative (**1**) via hydrazide intermediate (**4**). Mitsunobu reaction of **5** with ω-bromoalcohol provided compound (**6**). Combining **6** and monoalkoxynaphthol afforded **X-$_m$N$_n$Ox**. Similarly,

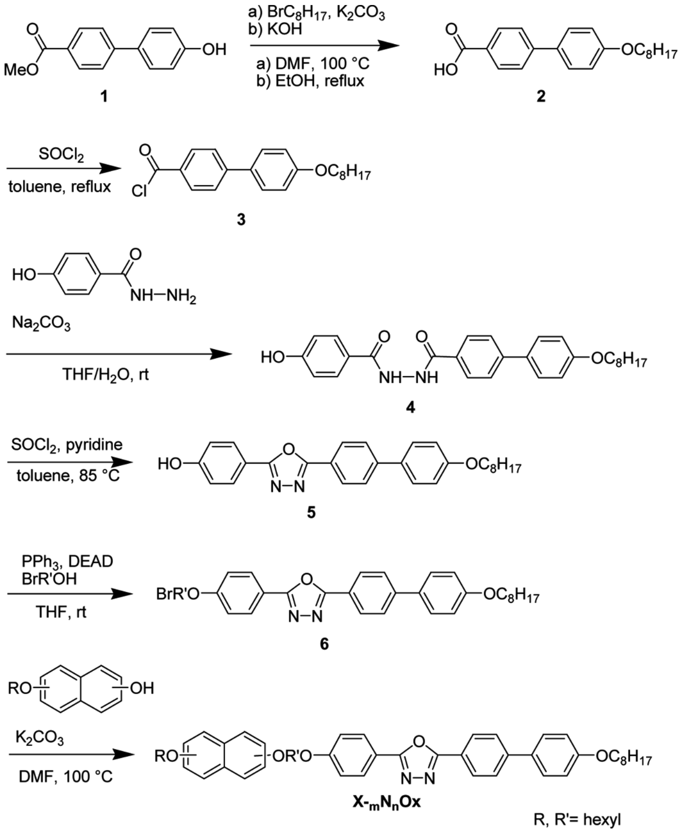

SCHEME 1 Synthetic route of $\mathbf{X\text{-}_mN_nOx}$.

cyanobiphenyl–naphthalene derivatives abbreviated as $\mathbf{X\text{-}_mN_nFCB}$ were synthesized by combining monoalkoxynaphthol (**9**) with 4'-(ω-hydroxyalkoxy)-3-fluoro-4-cyanobiphenyl using Mitsunobu reaction (Scheme 2). All compounds have certain lengths of alkyl chains as molecular terminals (m = 6) and as linkers between two cores (n = 6, 8).

Thermal Properties

Phase transition behaviors of $\mathbf{X\text{-}_mN_nOx}$ and $\mathbf{X\text{-}_mN_nFCB}$ were investigated by POM and DSC. The transition temperatures are summarized in Table 1. Figure 2 shows DSC traces of $\mathbf{15\text{-}_6N_6Ox}$, $\mathbf{26\text{-}_6N_8FCB}$ and $\mathbf{26\text{-}_6N_6FCB}$. All compounds showed thermotropic liquid crystalline

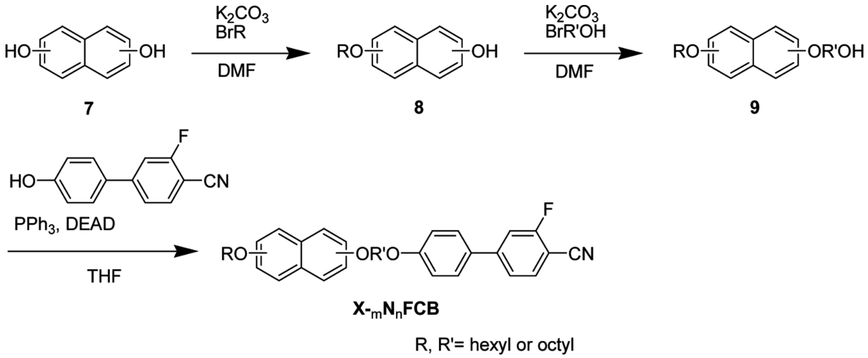

SCHEME 2 Synthetic route of **X-$_m$N$_n$FCB**.

behaviors and notable difference depending on the linkage position of the naphthalene core. **15-$_m$N$_n$Ox** showed enantiotropic phase transitions having smectic and nematic phases which were confirmed from the enthalpies of phase transitions indicated in the DSC chart (Figure 2) and the POM textures (a and b in Figure 3). On the contrary, **26-$_m$N$_n$Ox** and **27-$_m$N$_n$Ox** showed monotropic behaviors. This tendency is a quite contrast to behaviors of **X-$_m$N$_n$FCB**, *i.e.*, **15-$_m$N$_n$FCB** showed a monotropic phase transition while **26-$_m$N$_n$FCB** showed an enantiotropic one as well as previous results observed in **X-$_m$N$_n$CB** depicted in Figure 1 [18]. Relation between the linkage position of the naphthalene core and molecular shapes of the mesogen core might influence the phase stability. The phase transition temperatures of **X-$_m$N$_n$Ox** are higher than those of **X-$_m$N$_n$FCB**, while the transition temperatures observed in **X-$_m$N$_n$FCB** are lower than those of **X-$_m$N$_n$CB**. Generally, phase transition temperatures of liquid crystals are influenced by molecular interactions and crystallinity of

TABLE 1 Phase Transition Properties of **X-$_m$N$_n$Ox** and **X-$_m$N$_n$FCB**.

Compound	Transition temperature
15-$_6$N$_6$Ox	C 132 S 145 N 149 I
26-$_6$N$_6$Ox	C(142 S 155 N 171)^a 185 I
27-$_6$N$_6$Ox	C(129 N 132)^a 159 I
15-$_6$N$_8$FCB	C(61 N 71)^a 115 I
26-$_6$N$_6$FCB	C 98 S N 120 I
26-$_6$N$_8$FCB	C 89 N 111 I

^{a}Observed in a supercooling process.

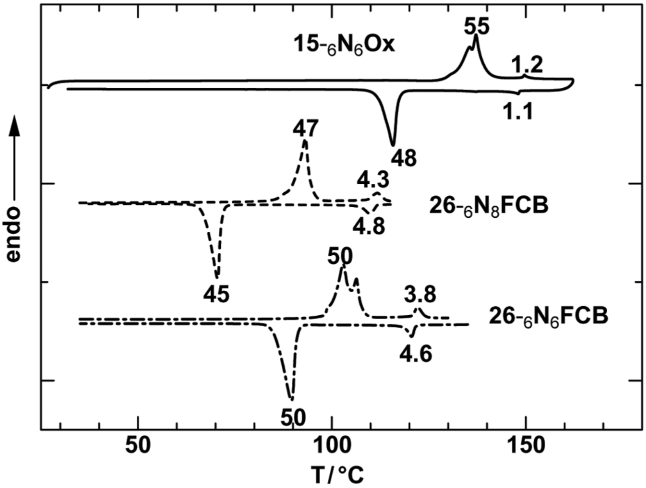

FIGURE 2 DSC traces and of **15-_6N_6Ox**, **26-_6N_6FCB** and **26-_6N_8FCB** and the phase transition enthalpies (kJ/mol).

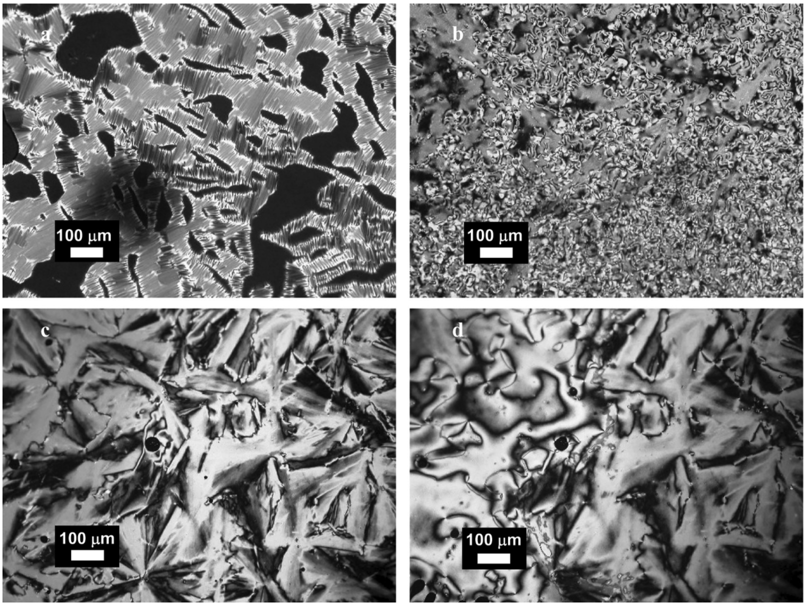

FIGURE 3 POM photographs of **15-_6N_6Ox** (**a**: smectic at 140°C, **b**: nematic at 145°C) and **26-_6N_6FCB** (**c**: smectic at 105°C, **d**: mixture of smectic and nematic at 110°C) in a heating process.

molecules. In this sense, introduction of the oxadiazole core that increases rigidness and planarity results in raise of phase transition temperatures. In contrast, monofluorination of the cyanobiphenyl core that decreases symmetry of molecules results in lowering of phase transition temperatures. At the same time, **26-$_m$N$_n$Ox** and **26-$_m$N$_n$FCB** showed the highest phase transition temperatures in each series, which suggests that **26-N** molecules could have the stronger molecular interaction than **15-N** and **27-N** molecules. It should be noted that the temperature ranges of mesophases of **X-$_m$N$_n$Ox** and **X-$_m$N$_n$FCB** are wider than **X-$_m$N$_n$CB** in most cases, and distinct smectic phases can be observed in certain cases (Figure 3).

Optical Properties

We chose **15-$_6$N$_6$Ox** and **26-$_6$N$_8$FCB** to investigate their optical properties, because they showed enantiotropic behaviors with distinct phase transitions. The optical properties in each state were investigated by UV-vis and photoluminescence (PL) spectroscopies equipped with a temperature controller. Their optical properties are summarized in Table 2. All compounds showed bluish fluorescences in the crystal, liquid crystal and isotropic liquid states, respectively. Figures 4 and 5 show the UV-vis and PL spectra of **15-$_6$N$_6$Ox** and **26-$_6$N$_8$FCB**, respectively. In the UV-vis spectra in the solution state, **15-$_6$N$_6$Ox** showed absorption peaks at 316 and 326 nm. These peaks are attributed to absorptions at 1,5-dialkoxynaphthalene portion. On the other hand, **26-$_6$N$_8$FCB** showed a single peak at 306 nm with a small shoulder at 346 nm. In this case, this shoulder is due to an absorption at the 2,6-dialkoxynaphthalene portion.

In the PL spectra of **15-$_6$N$_6$Ox**, an emission peak was observed at 387 nm in the solution and at 398 nm in the crystal state, respectively. The PL spectrum of **15-$_6$N$_6$Ox** in the liquid crystal state was similar to that in the crystal state. Since we have preliminarily confirmed that

TABLE 2 The Optical Properties of **15-$_6$N$_6$Ox**, **26-$_6$N$_8$FCB** and **N–FCB**.

	UV-vis ($\lambda_{\max}$) nm	PL ($\lambda_{\max}$) nm			
Compound	in $CHCl_3$	in $CHCl_3$	crystal	liquid crystal	isotropic liquid
15-$_6$N$_6$OX	316, 326	387	398, 410	401	–
26-$_6$N$_8$FCB	306 (346)	364	424	459	457
N–FCB	304 (346)	363	420	–	458

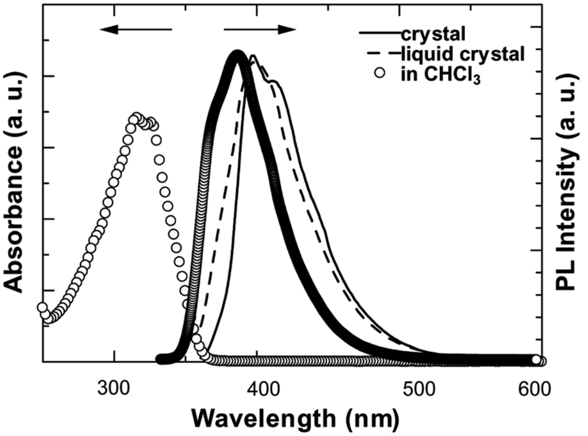

FIGURE 4 PL spectra of **15-$_6$N$_6$Ox** in the crystal state (solid line), in the liquid crystal state (broken line) and UV-vis and PL spectra in $CHCl_3$ solution (open circle).

1,5-dialkoxynaphthalene showed an emission peak at around 480 nm in the crystal state, the red shift observed in **15-$_6$N$_6$Ox** is trivial. This result indicates that introduction of the large oxadiazole core suppresses the excimeric interaction between the naphthalene moieties. On the other hand, the PL spectra of **26-$_6$N$_8$FCB** exhibited significant changes through phase transitions, *i.e.*, the emission peak in the

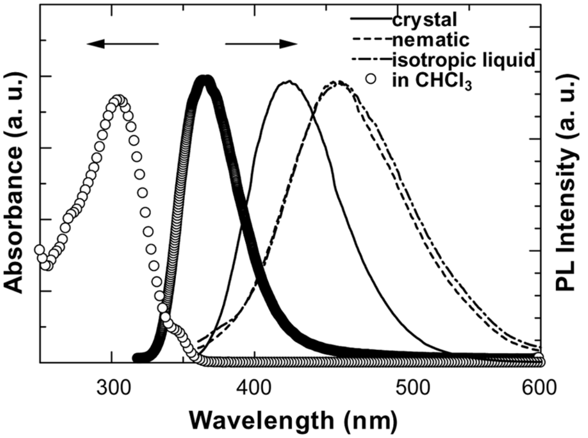

FIGURE 5 PL spectra of **26-$_6$N$_8$FCB** in the states of crystal (solid line), nematic (broken line), isotropic liquid (dot-dashed line), and UV-vis and PL spectra in $CHCl_3$ solution (open circle).

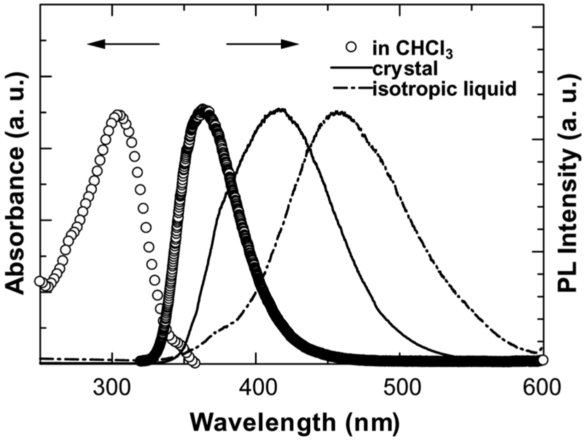

FIGURE 6 UV-vis and PL spectra of **N–FCB** in the states of crystal (solid line), isotropic liquid (dot-dashed line), and UV-vis and PL spectra in $CHCl_3$ solution (open circle).

solution state observed at 364 nm largely red-shifted to 424 nm in the crystal state. Furthermore, emission peaks in the liquid crystal and isotropic liquid states were observed in a region of longer wavelength at 459 nm and 457 nm, respectively. These results indicate that molecular interactions similarly work between **26-$_6$N$_8$FCB** molecules in the solid, liquid crystal and isotropic liquid states. To investigate what interaction led to the significant red shifts, we prepared a mixture sample (50/50 mol%) of 2,6-dialkoxynaphthalene and 4′-octyloxy-3-fluoro-4-cyanobiphenyl (**N–FCB**) and compared the UV-vis and PL spectra. Because **N–FCB** only exhibited an unstable monotropic phase transition in the supercooling process, we could obtain UV-vis and PL spectra in solution, crystal and isotropic liquid states (Fig. 6). It is interesting to note that the optical data of **N–FCB** well agree with those of **26-$_6$N$_8$FCB**. Since the characteristic red-shifts observed in **N–FCB** during the phase transitions have never been observed 2,6-dialkoxynaphthalene and 4′-octyloxy-3-fluoro-4-cyanobiphenyl by themselves, it is concluded that there is a specific interaction between electron rich dialkoxynaphthalene and electron deficient fluorocyanobiphenyl cores.

CONCLUSIONS

In this study, we succeeded to synthesize luminescent naphthalene-based liquid crystals having oxadiazole and fluorocyanobiphenyl cores.

Our objective is to synthesize novel luminescent liquid crystals showing a remarkable spectral change through distinct phase transitions. **X-$_m$N$_n$Ox** and **X-$_m$N$_n$FCB** showed notable differences of phase transition behaviors depending on the linkage positions of the naphthalene core. **15-$_6$N$_6$Ox**, **26-$_6$N$_6$FCB** and **26-$_6$N$_8$FCB** showed enantiotropic behavior and their mesopheses were observed in the distinct temperature regions. The phase transition temperatures of **X-$_m$N$_n$Ox** series were higher than those of **X-$_m$N$_n$FCB** series, which is due to the rigid conjugated structure of the oxadiazole portion. All compounds showed bluish emission in the crystal, liquid crystal and isotropic liquid states. Especially, we observed that **15-$_6$N$_6$Ox** showed little PL spectral change through phase transitions but **26-$_6$N$_8$FCB** showed remarkable red shifts in the liquid crystal and isotropic liquid states. From these results, it is obvious that there is little molecular interaction between oxadiazole and naphthalene cores in **15-$_6$N$_6$Ox** but the specific interaction is present between fluorocyanobiphenyl and naphthalene cores in **26-$_6$N$_8$FCB**. With this study, the materials having change of PL colors through phase transitions will be initiated to develop as a new class of luminescent materials.

REFERENCES

[1] O'Neill, M. & Kelly, S. M. (2003). *Adv. Mater.*, *15*, 1135.

[2] Lüssem, G. & Wendorff, J. H. (1998). *Polym. Adv. Techol.*, *9*, 443.

[3] Tokuhisa, H., Era, M., & Tsutsui, T. (1998). *Appl. Phys. Lett.*, *72*, 2639.

[4] Kogo, K., Goda, T., Funahashi, M., & Hanna, J. (1998). *Appl. Phys. Lett.*, *73*, 1595.

[5] Attias, A.-J., Cavalli, C., Bloch, B., Guillou, N., & Noël, C. (1999). *Chem. Mater.*, *11*, 2057.

[6] Strehmel, B., Sarker, A. M., Malpert, J. H., Strehmel, V., Seifert, H., & Neckers, D. C. (1999). *J. Am. Chem. Soc.*, *121*, 1226.

[7] Levitsky, A., Kishikawa, K., Eichhorm, S. H., & Swager, T. M. (2000). *J. Am. Chem. Soc.*, *122*, 2474.

[8] Sentman, C. & Gin, D. L. (2001). *Adv. Mater.*, *13*, 1398.

[9] Kawamoto, M., Mochizuki, H., Ikeda, T., Lee, B., & Shirota, Y. (2003). *J. Appl. Phys.*, *94*, 6442.

[10] Lam, J. W. Y. & Tang, B. Z. (2003). *J. Polym. Sci. A: Polym. Chem.*, *41*, 2607.

[11] Giménez, R., Pinõl, M., & Serrano, J. L. (2004). *Chem. Mater.*, *16*, 1377.

[12] Hulvat, J. F., Sofos, M., Tajima, K., & Stupp, S. I. (2005). *J. Am. Chem. Soc.*, *127*, 366.

[13] Abraham, S., Mallia, V. A., Ratheesh, K. V., Tamaoki, N., & Das, S. (2006). *J. Am. Chem. Soc.*, *128*, 7692.

[14] Chung, S.-F., Wen, T.-C., Chou, W.-Y., & Guo, T.-F. (2006). *Jpn. J. Appl. Phys.*, *45*, L60.

[15] Aldred, M. P., Eastwood, A. J., Kelly, S. M., Vlachos, P., Contret, A. E. A., Farrer, S. R., Mansoon, B., O'Neill, M., & Tsai, W. C. (2004). *Chem. Mater.*, *16*, 4928.

[16] Lin, H.-C., Lee, K.-W., Tsai, C.-M., & Wei, K.-H. (2006). *Macromolecules*, *39*, 3808.

[17] Hwang, D. H. & Shim, H. K. (2002). *Thin. Solid. Films*, *417*, 166.

[18] Mori, T. & Kijima, M. (2007). *Chem. Lett.*, *36*, 710.